ISSN 1061-9348, Journal of Analytical Chemistry, 2016, Vol. 71, No. 11, pp. 1069–1080. © Pleiades Publishing, Ltd., 2016.
Original Russian Text © Yu.K. Shazzo, Yu.A. Karpov, 2016, published in Zhurnal Analiticheskoi Khimii, 2016, Vol. 71, No. 11, pp. 1123–1136.

REVIEWS

Laser Sampling in Inductively Coupled Plasma Mass Spectrometry in the Inorganic Analysis of Solid Samples: Elemental Fractionation as the Main Source of Errors

Yu. K. Shazzo[a, *] and Yu. A. Karpov[b, c, **]

[a] *All-Russian Research Institute for Optical and Physical Measurements, Moscow, 119361 Russia*
[b] *GIREDMET State Research and Design Institute of Rare Metal Industry, Moscow, 119017 Russia*
[c] *National University of Science and Technology MISIS, Moscow, 119049 Russia*
**e-mail: uksh@narod.ru*
***e-mail: karpov@giredmet.ru*

Received September 16, 2015; in final form, May 5, 2016

Abstract—The review is devoted to one of currently most often used methods for the study of the elemental composition of samples differing by origin and matrix, laser sampling (**LS**), in combination with inductively coupled plasma mass spectrometry. The method ensures the analysis of samples without their transfer into solution and with high spatial resolution, up to several micrometers. The main restriction of laser sampling is due to elemental and isotopic fractionation, proceeding in the interaction of laser irradiance with the sample surface, on which photoelectronic and thermal processes, resulting in the formation of sample aerosols of different nature, can occur depending on the characteristics of laser irradiance. The paper covers works on the study of the effect of the laser wavelength, pulse duration, pulse fluence, plasma screening, explosive boiling, and the crater geometry on elemental fractionation and works in which fractionation coefficients were calculated on the basis of experimental data.

Keywords: inductively coupled plasma mass spectrometry, laser sampling, laser pulse, elemental fractionation, elemental fractionation

DOI: 10.1134/S1061934816110125

Many instrumental methods of chemical analysis of different samples require the preliminary transfer analytes into solution. Such procedures are often associated both with problems of the dissolution of samples of complex composition and with a possibility of their contamination with impurities present in the reagents, which introduces significant errors into the results of analysis. The development of methods of the introduction of solid samples into analytical instruments was always an urgent problem of methodological research conducted by analytical chemists. A successful solution of these problems was provided by the laser sampling (**LS**) of solid samples. The LS method in combination with inductively coupled plasma mass spectrometry (**LS–ICP–MS**) appeared a rapid technique for the direct elemental and isotope analysis of any solid sample with minimum preparations to the analysis without the transfer of solid samples into solution and, in most cases, without the introduction of additional reagents. In addition, the method offers a possibility of the *local* analysis of solid and liquid microscopic inclusions and gives spatial information about the composition of elements. Determination by MS ensures the positive identification of elements with lower spectral noises compared to atomic emission spectroscopy (**AES**). From several pico- to several femtograms of a sample are sufficient for recording an analytical signal, depending on the sensitivity of the used analytical equipment. These values are much lower than those typical for methods utilizing the injection of sample solutions through a nebulizer chamber. The rapid development of LS–ICP–AES(MS) methods considerably increased interest of researchers in these analytical techniques for the determination of a great number of elements with very low limits of detection [1–6]. The methods have found application both in scientific academic and applied research, including those in ecological, geological, metallurgical, archaeological, judicial, semiconductor, medicobiological, etc. branches [7]. Nevertheless, the drift of the analytical signal observed with all types of lasers and samples with different matrices, so-called "elemental fractionation" appeared to be one of the main problems in LS–ICP–MS. This phenomenon may be due to different extents associated with LS, transportation, or excitation and ionization processes in inductively coupled plasma. The accuracy of the results of analysis is directly related to

the successful overcoming of elemental fractionation or with its account in recording and processing of the results.

In foreign scientific periodical literature, processes of laser sampling were described in different terms, for example "laser probe," "laser microprobe," "laser sampling," or "laser ablation." However, the term "laser ablation," which was copied in Russian literature as "lasernaya ablyatsiya," has occupied the dominant position and could assimilate in it, although many scientists often notice their rejection of this term. The word "ablation" has Latin origin and means "to carry mass away." We will try to avoid this expression invaded into Russian and quite dissonant and use the term "laser probe sampling," or "laser sampling" with the abbreviation "LS."

The first use of LS as a method of sample injection into ICP–MS was described by Gray in 1985 [8]. At the energy of laser pulse 0.5–1 J, craters 0.5–0.7 mm in diameter and depth formed for 0.2-mg samples and pulses of the energy 0.5 J, and the limits of detection were reduced to 10 ng/g. Later LS as a method of sample injection into ICP–MS was used and described by many authors [9–14]. The further development of the local microanalysis of solid samples using LS led to the reduction of diameters of the formed craters to 10 μm and smaller and allowed analysts to conduct research with spatial resolution up to 4 μm [1, 10, 15–21]. Today LS–ICP–MS as the most widespread and available microprobe is used for the local microelemental quantitative analysis of different solid samples.

Lasers for sampling. In the early years, ruby and carbon dioxide lasers with high pulse energies were used for elemental analysis with LS [2, 7, 22, 23]. Later solid-state lasers based on yttrium aluminum garnet with a neodymium dopant (Nd:YAG), titanium–sapphire lasers (Ti–Al_2O_3), and excimer lasers utilizing noble gas (Ar, Kr or Xe) mixtures with chemically active gases fluorine or chlorine [4, 6, 24–32] accepted the widest distribution for laser sampling in elemental analysis.

Inductively coupled plasma as an ion source. In inductively coupled plasma, aerosol particles moved with carrier gas flow from the LS place are vaporized, atomized, and ionized. Elemental fractionation can result from the incomplete dissociation of sufficiently large particles on their injection into ICP; therefore, the formation of smaller particles on the interaction of laser irradiance with a sample surface favors not only their more complete drift to the plasma but also the higher probability of their complete ionization. The role of ICP as an ion source was described in numerous papers [for example, 33–37]. For the first time, ICP was successfully used in combination with quadrupole mass analyzers in [38–40]. The detailed description of functions and characteristics of all ICP–MS systems can be found, for example, in [35, 36, 41].

Effect of laser irradiance parameters on LS. Laser irradiance parameters along with the nature of the studied sample and other factors strongly affect elemental fractionation, because they determine the quality of aerosols formed by laser sampling. The aerosols must consist of sufficiently small particles with a uniform fractional and chemical composition, independent of their size. Elemental fractionation in the LS site can be minimized by optimizing the conditions of laser impact: wavelength, pulse duration, intensity, and frequency [42].

Advantages of UV radiation over IR radiation in LS. Laser wavelength considerably affects sampling, because, at shorter wavelengths, the energy of laser irradiance is absorbed more efficiently, and bond breaks and ionization of solid substances proceed more efficiently because of the higher energy of photons. Wavelength plays a particularly important role in sampling by nanosecond laser irradiance. It was found that among the advantages of UV lasers over IR ones are the overcoming of matrix effects and the better stoichiometric representativity of the ablated samples; the reduction of plasma screening; more efficient interaction of laser irradiance with the sample surface; the reduction of spatial resolution up to 4 μm; high sensitivity; and possibility of analyzing any solid sample, including transparent ones [21, 43, 44]. It was shown that the shorter laser wavelength led to the higher rate of sampling and the lower fractionation [6, 13, 24, 45–48]. A comparison of the most often used UV wavelengths, 266, 213, and 193 nm, of the Nd:YAG-laser and also 157 and 193 nm of the excimer laser showed that laser irradiance of the deep UV (DUV) region (157 and 193 nm) is most suitable for LS, because it is absorbed by the majority of samples and produces small particles, which particle size distribution is the least dependent on the matrix and which are easily moved with the carrier gas and efficiently atomized and ionized in the ICP. Hence, laser irradiance with wavelengths shorter than 213 nm was recommended for use in LS–ICP–MS [13, 49–51].

Effect of pulse duration on LS. It was found that rather strong fractionation in the LS of brass at 30 ns (248 nm) in an argon atmosphere was insignificant for LS with 35 ps pulses (266 nm) [52], and that the dominant process for the 3 ns Nd:YAG-laser and the 30 ns pulses of excimer laser for power densities below 0.3 GW/cm^2 was thermal evaporation, whereas at 35 ps, the nonthermal mechanism (see below) was prevailing in LS at all three wavelengths 1064, 532, and 266 nm, which points to the best suitability of the picosecond UV laser for elemental analysis [53].

Le Harzic et al. [54] observed the dependence of LS thresholds and the depth of penetration of laser energy on pulse duration in the range from 100 fs to 5 ps. Increasing pulse duration enhanced the threshold fluence and reduced the penetration depth of effective energy. It was also shown that thermal pro-

cesses proceeded even in the femtosecond region and deteriorated the quality, accuracy, and efficiency of the LS of substances.

When comparing 370-fs and 5-ns LS, Perdian et al. showed that shorter pulses considerably reduced the frequency and amplitude of signal spikes in ICP–MS due to the evaporation, atomization, and ionization of large particles, which were the main reasons for fractionation in ICP–MS [55]. It was also shown that near IR (NIR) femtosecond LS (785 nm, 130 fs) weakly depended on matrix effects and elemental fractionation was much weaker or absent compared to nanosecond LS, depending on the element [56]. Freydier et al. [57] showed that analytical characteristics of measurements at IR pulses (800 nm) improved by a factor of up to 4 with transition from picosecond to 60 fs pulses, while no improvement was observed at 266 nm.

Comparing three LS–ICP–MS systems (213 nm nanosecond, 193 nm nanosecond, and 200 nm femtosecond) in the analysis of sulfide minerals [58], Wohlgemuth-Ueberwasser did not observe melting of any of sulfides using femtosecond LS in contrast to nanosecond ones. Matrix effects in femtosecond LS were insignificant. The majority of fractionation indices (FI) were near unity for all three LS systems. Elemental fractionation appeared to be independent of the LS process and an increase in the crater depth, and the uncertainties in FI were related to the nonuniform distribution of platinum-group metals in a corresponding sample rather than to elemental fractionation in the crater.

Poitrasson et al. [59] showed an advantage of UV fs over ns LS–ICP–MS at 266 nm for decreasing of chemical fractionation due to thermal processes (see below), resulted in more precise, better reproducible, and more accurate elemental (Pb/U, Pb/Th) ratios and lead isotopic ratios. Femtosecond calibration of LS–ICP–MS was less dependent on the matrix matching and, therefore, more universal. Pulse duration didn't effect on elemental ratios $^{206}Pb/^{238}U$ and $^{208}Pb/^{232}Th$ in monazite in the range 60–300 fs, noticeable matrix effects were not revealed either [60]. In comparing 150 fs and 15 ns LS–ICP–MS using wavelengths of 795, 265, and 193 nm for the analysis of SRM NIST612, BCR-2G, GSE-1G, and BAM-S005A Ohata et al. showed in [61] that fs LS did not ensure the accuracy of analysis improved in comparison with ns LS, especially in the analysis of opaque samples and in using DUV laser irradiance. In addition, element concentrations for glasses agree with the certified values even better in DUV-ns-LS than in NIR fs LS–ICP–MS and the use of DUV fs LS systems is always preferable in the analysis of samples with a wide variety of matrices.

The advantages of femtosecond over nanosecond UV (196 nm) LS for the determination of the isotope ratios of heavy stable isotope systems were considered in [26, 62–65]. In using nanosecond UV pulses, substantial isotope fractionation, introducing noticeable errors in the determination of the isotope ratios of heavy metals, for example $^{56}Fe/^{57}Fe$ [66] and $^{65}Cu/^{63}Cu$ [67] was observed. The authors of works [26, 68] supposed that isotopic ratio shifts were due to irregular and irreproducible conditions of LS, such as thermal deformations (see below) and particle size distribution influence. To overcome the problems of nanosecond LS, it was proposed to use fs lasers working at 196 or 266 nm. Studies [62–64, 69] of the isotopic composition of Fe and Si in silicate matrices supported observations [26] of the substantial independence of the UV fs LS–ICP–MS method of matrix effects and of a possibility of using standard samples (SRM) without matrix matching.

Shaheen et al. [42] showed that fs laser irradiance produced more intense and stable ICP–MS signals in comparison with ns LS, despite lower power and smaller craters, (30 mJ and ~35 μm in diameter for 130 fs; 800 mJ and ~85 μm in diameter for 8 ns) because of the formation of much smaller particles with more uniform particle size distribution. In comparing [70, 71] 130 fs and 110 ps LS of electrolytic iron and SRM NIST 610 of glass and SRM 1107B of brass, researchers in both cases revealed the presence of thermal effects at high laser fluences; however, at low laser fluences, thermal effects were insignificant for fs LS. In addition, fs LS gave particles of smaller size in comparison with those obtained by ps LS. A dependence of elemental fractionation on pulse frequency was found. Elemental ratios measured for $^{66}Zn/^{63}Cu$, $^{208}Pb/^{238}U$, $^{232}Th/^{238}U$, $^{66}Zn/^{232}Th$, and $^{66}Zn/^{208}Pb$ changed with the number of laser pulses at both pulse durations; however, the reproducibility, fractionation, and element ratios in themselves were much better for fs pulses (RSD ~3–6%) than for ps pulses (RSD ~ 7–11%).

Physical processes in laser-induced plasma. *Thermal and nonthermal processes.* Laser systems with pulse duration from 100 fs to several ns allowed the researchers to perform the detailed analysis of the interaction of laser pulses of different duration with the substance at the invariance of other characteristics of laser irradiance and to explain the almost complete absence of elemental fractionation in these cases. A number of works, for example [6, 72, 73], demonstrated that the interaction of laser irradiance with the sample surface may include, depending on the wavelength and duration of laser pulses, both thermal and nonthermal mechanisms and also their combinations.

Works considering characteristics of the LS of metals in a low fluence regime at femto-, pico-, and nanosecond laser pulses were summarized in [74]. The conditions were determined by the electron cooling times, the lattice heating time, and pulse duration. It was shown in [75–77] that the process of sampling by fs and ps pulses can be considered a direct phase transi-

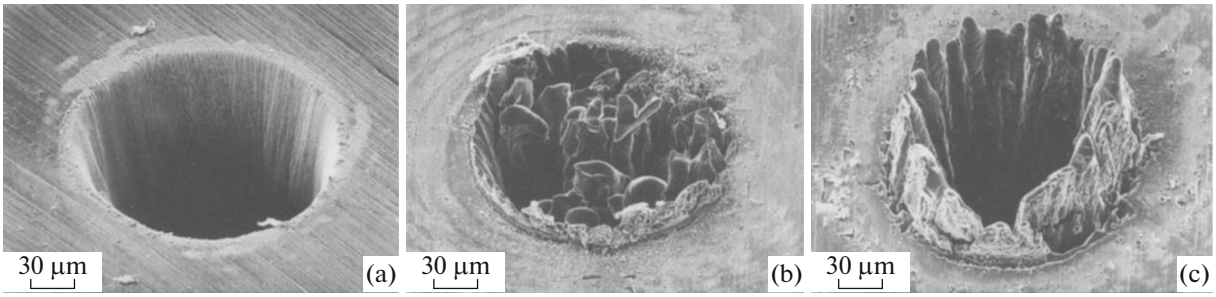

Fig. 1. Laser sampling craters in steel foil 100 μm thick using laser pulses at 780 nm: (a) 200 fs, 120 μJ, $F = 0.5$ J/cm^2; (b) 80 ps, 900 μJ, $F = 3.7$ J/cm^2; (c) 3.3 ns, 1 mJ, $F = 4.2$ J/cm^2 [74].

tion of a solid substance to vapor (or plasma) with the minimum fractionation. Evaporation from the liquid phase at nanosecond pulses occurs under the action of thermal processes; it results in the transfer of substance both to vaporous and liquid phases. The difference in the heats of phase transition in the evaporation of different chemical elements in thermal processes can induce strong fractionation [6].

Figure 1 shows craters obtained in [74] under the action of laser irradiance with a fluence of 0.1–5 J/cm^2 on a 100-μm thick steel foil with 10^4 laser pulses in fs, ps, and ns modes and clearly demonstrates results of thermal processes in the transition from fs to ns pulses.

Stuart et al. in [78] showed that, for laser pulses up to 10 ps at 1053 and 526 nm, the LS of quartz glass and calcium fluoride proceeded due to the rapid formation of plasma and the removal of the surface layer, and for pulses longer than 100 ps, due to usual melting and boiling. A conclusion was drawn in [79] that the LS of oxide ceramics (Al_2O_3, MgO, ZrO_2) with fs and ps laser pulses can be considered a direct transition of a solid substance into vapor.

As was shown [72, 80] for the ps LS of silicon, the main mechanism of electron emission from the surface for laser fluences below the melting threshold is the emission of photoelectrons (nonthermal process), whereas thermionic emission (thermal process) can occur near the melting threshold.

In the conditional time scale (Fig. 2) [81], one can see stages of absorption of laser energy and substance ablation in ns and fs modes of laser pulse duration and processes proceeding under these conditions. In the fs LS, plasma formed after the termination of the laser pulse, while in ns LS, it formed during the laser pulse with part of pulse energy consumed for repeated plasma heating. It was shown that the lifetime of the plasma was longer for ns LS compared to fs LS. It appeared that elemental fractionation was not observed in the range of pulse durations from 40 fs to 1 ps, which could significantly improve the analytical characteristics of the LS–ICP–MS method.

The authors of works [82–86] showed that thermal processes occurring in ns LS can include normal evaporation, normal boiling, and explosive boiling. The last process remains the only thermal mechanism that can explain laser sputtering at high fluences [84] and is a factor responsible for the inhomogenous transition of sample matter to the vapor and, therefore, for errors in the results of analysis. The detailed theoretical model and a possible mechanism of explosive boiling were described in [87–89]. It was shown that, for wider beams and longer wavelengths of laser irradiance, higher density of laser irradiance is required for phase explosion.

Plasma screening. Processes of plasma screening, studied in a number of works, e.g. [90–97], in which the laser beam could interact with an expanding plasma torch produced at an early stage of LS, depending on the pulse duration, also strongly depended on the laser wavelength. Depending on the wavelength, laser irradiance can be intensely absorbed or reflected by the plasma. Photon of short-wave UV radiation more efficiently penetrate into plasma and directly initiate bond breaks in a sample, which results in a higher rate of LS and smaller fractionation, and, therefore, in smaller errors and better reproducibility of elemental analysis with LS. As was shown in [98], high-energy photoelectrons emitted from a copper sample in passing the leading edge of the wave of a ps laser pulse form plasma in the gas over the target while absorbing inverse bremsstrahlung. The degree of plasma expansion depends on the gas properties. The absorption of plasma in the ps LS of a solid substance can be reduced using either an ambient gas environment with a high ionization energy or low gas pressure. On an example of a brass sample, Kuhn et al. showed in [99] that, under the conditions of laser-induced plasma, heating and partially evaporating emitted particles, the gas phase at this stage was enriched and the particles were depleted with zinc.

Amoruso et al. [94] found out that a laser beam of low fluence passed to the target almost without attenuation by the formed vapor. Heat transfer resulted in the melting and evaporation of the target. For laser irradiance exceeding the fluence threshold (≥2 J/cm^2), the temperature of the vapor was rather high to cause noticeable atomic excitation and ioniza-

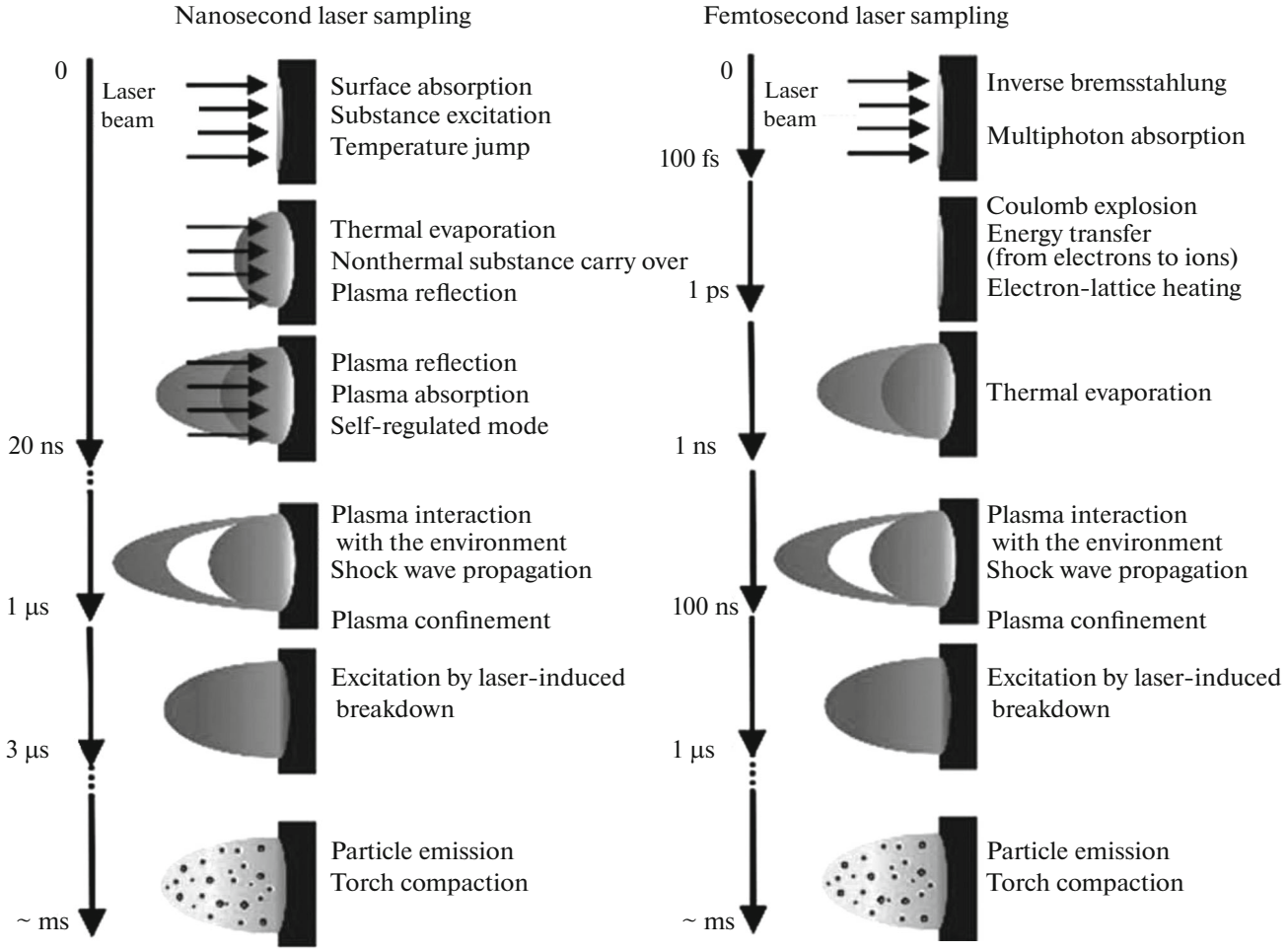

Fig. 2. Approximate time intervals in energy absorption and substance ablation along with processes occurring for 50 fs and 10 ns LS [81].

tion of atoms, after which the vapor started to absorb incident laser irradiance, which, in turn, resulted in the decomposition of vapor and the formation of plasma. As was shown in [93, 100], depending on the wavelength of laser irradiance, electron density, plasma sizes, and its electron temperature, the target can be efficiently shielded from laser pulses, up to the total reflection of the laser beam, which results in the reduction of the interaction of laser irradiance with the sample and, consequently, in a decrease in the amount of laser ablated substance with an increase in fractionation. Eggins et al. showed in [47] that the high laser fluence could lead to an increase in the contribution of the plasma sampling of the target matter, which can become the prevailing process, significantly increasing fractionation at a rather high pulse energy.

Effect of laser intensity. Laser fluence is also an important factor affecting the productivity and quality of LS–ICP–MS, because it determines the degree of elemental fractionation [6, 42]. The dependence of the processes of melting, explosive boiling, and substance ablation, responsible for elemental fractionation, on the density of laser fluence was investigated in [54, 101, 102]. It was shown that in the low fluence regime penetration depth is close to the theoretical depth of optical penetration and the thresholds of LS are quite low; at higher fluences, the efficient penetration depth increased from 10- to 20-fold and LS thresholds also increased. Shaheen et al. distinguished four threshold transitions characterizing changes in the prevailing LS mechanism for different ranges of laser fluence: the beginning of LS, screening by ionized mass, explosive mass ablation, and screening by electron plasma [42]. They described in detail changes in the degree of fractionation depending on the intensity of laser irradiance and physical mechanisms of processes responsible for elemental fractionation. As was shown in [103], the dependence of elemental fractionation on the density of laser fluence is individual for each sample, because, for samples optically transparent at the given wavelength, high intensity laser fluences are required, whereas for samples with high heat conductivity and low melting points, low intensities are required even at fs pulses. When the laser fluences considerably exceed

the LS threshold for particular samples, e.g., for standard samples of brass, Al, and silicate glass >5 J/cm^2, elemental fractionation becomes insignificant [104].

It was shown in [105] that elemental fractionation in LS, both for nanosecond and femtosecond lasers, could be reduced if the laser fluence was much higher than the LS threshold for the irradiated sample. However, preferable evaporation and losses in the diffusion of volatile elements from the melt in the crater (for ns LS and metal samples) will be present, but can be reduced using low-intensity and low-frequency pulses.

Different mechanisms of processes of the evaporation of the target substance in the range of laser intensities 200–350 MW/cm^2 were considered in [106]. It was also shown in [107–109] that normal evaporation from an irradiated surface occurred at the laser fluence below 5.2 J/cm^2 and explosive phase transition prevailed in the course of evaporation at laser fluences higher than 5.2 J/cm^2. The study of the composition of glass aerosols formed in NIR fs LS (200–250 fs) [100] showed that the concentrations of Ca, Zn, Sr, Ba, and Pb in them corresponded to that of the bulk material if the selected laser fluence considerably exceeded 5 J/cm^2. However, for the LS of metals, intensity should not be higher than 5 J/cm^2 because of elemental fractionation and intense formation of micrometer particles. In addition, it was shown that, at shorter pulses (<150 fs), the stoichiometric sampling of brass was possible for fluences up to 50 J/cm^2. However, the data [110] indicate that, in the LS of brass (785 nm; 130 fs), the direct transfer of the solid substance to vapor with the formation of small particles of nanometer sizes proceeded at fluences <19.14 J/cm^2, and, at fluences of >20.47 J/cm^2, the ejection of molten substance droplets was observed, which points to the prevalence of thermal processes.

It was shown [111], that in the LS of glass (266 nm, 5 ns), laser power density of 0.4–0.5 GW/cm^2 was the threshold value for changing of the particle size distribution of the aerosol towards the formation of smaller particles, plasma screening, and the ablation rate of many materials.

Elemental fractionation. The main source of errors in measurements of concentrations of elements, isotopes, and isotope ratios by LS–ICP–MS is provided with fractionation effects. The first type of fractionation relates to space charge effects in the ICP region and also in the expansion chamber between the sampling and scimmer cones. This effect favors the scattering of light isotopes from the ion trajectory. The second type of fractionation occurs in the region of the sampling cone and system of focusing lenses and depends on ion energy, which, in turn, depends on the element. The third type of fractionation, which we call fractionation in LS, makes the main contribution to the instability of measurements by LS–ICP–MS [112]. This source of fractionation is arranged in the place of target irradiation and affects the degree of fractionation, which may occur at the further steps of the process, both during the transportation of the aerosol and in the evaporation and ionization of the transferred particles and aggregates. Just this type of fractionation will be considered further in more detail.

Elemental fractionation was considered by many authors for all types of lasers, including fs ones, and for different wavelengths of laser irradiance [see, e.g., 4, 47, 51, 113–116]. A considerable decrease in elemental fractionation with UV lasers in comparison with IR lasers was shown; however, the complete elimination of matrix effects was not attained. As was noted in [116–118], the degree of elemental fractionation may be determined by the redistribution of elements between the phases formed in the region of the crater in the course of laser heating and sample evaporation, differences in the degrees of element evaporation from the melt in the crater region because of differences in their volatilities, fractional condensation of vapors with the formation of refractory element condensates, gravity sedimentation or the diffusion of particles in the substance transfer to the ICP, incomplete evaporation and ionization of big particles (larger than 150 nm) with an increase in the MS signal from more volatile elements, the suppression of the signal of volatile elements in the plasma by the big masses of aerosols (mass load). All these factors can be responsible for the distortion of the measured concentrations of elements and isotopes.

Mass transfer based on thermophysical properties, accompanied by elemental fractionation depending on the physical and chemical properties of the sample and characteristics of laser irradiance during the laser pulse, was noted in [21, 28, 47, 53, 113, 114, 117–129]. Elemental fractionation depending on the position of the target inside the LS chamber was also observed in [130] and related to distinctions in the behavior of refractory and volatile elements during condensation from laser-induced plasma and correlated with the local velocity of helium rather than with the interaction of laser irradiance with the solid sample. Studies [117, 131] demonstrated that elemental fractionation and matrix effects due to mass load in LS at 213 and 193 nm with Nd:YAG lasers were insignificant for refractory litophile elements, particularly, for the 193 nm laser (<5%). However, for chalcophile and siderophile trace elements with low boiling points, these effects were up to 40 and 20% for 213 and 193 nm lasers, respectively, and nonstable for NIST glasses and carbonates. Besides, the effect of mass load was much weaker for laser irradiance with the wavelength 193 nm.

In a number of studies, for example [111, 132, 133], it was shown that the sizes of particles formed in the LS of aerosols strongly affect the efficiency of evaporation and ionization in the ICP; for sufficiently large sizes of particles, the evaporation and ionization pro-

ceeded incompletely, resulted in elemental fractionation, and affected the analytical characteristics of ICP-MS. The size, fractional, and chemical composition of the ablated particles directly depended on the wavelength, power density, beam diameter, and pulse duration of laser irradiance, and also on sample matrix and ambient gas. Smaller particles from fs LS resulted in an increased intensity and stability of the ICP–MS signal in comparison with ns LS. However, the dependence of element distribution in aerosols on particle size was different for different elements. As was shown on an example of the LS of brass samples in [99], copper and zinc in the aerosol were distributed heterogenously: particles larger than 100 nm were enriched with copper up to 100% and particles of the size <100 nm and vapor phase were enriched with zinc by more than for 40%. In the study of the fs LS of an intermetallic NiAl compound, Jorgensen et al. showed that nanoparticles of the size 1–30 nm were amorphous and enriched with aluminum, while larger particles (>100 nm) were crystalline and depleted with aluminum [134].

A dependence of the sizes of particles and aggregates formed in the aerosol in the LS on gas flow rate at the LS place was shown in [135]: larger particles and aggregates formed in the zones of the low flow rate of helium, which led to the incomplete evaporation and depletion of the aerosol with refractory elements in the ICP. To reduce fractionation, Guillong et al. removed almost all particles larger than 0.8 μm [136]. However, as was shown in [99], elements in LS were distributed heterogenously within the various particle size fractions. For this reason, large particles must not be removed from the aerosol, because this could change its overall stoichiometry.

As was shown in [137], the LS of biogenic carbonates and NIST SRM 612 gave micro- and nanosized particles. This distinction was determined by the method of their formation: in the laser sampling of silicates (NIST 612), microparticles formed by hydrodynamic spraying, while in the sampling of biogenic carbonates, by a photomechanical breakdown. The effect of these distinctions can be minimized using a 193 nm laser, which gave smaller particles than the 213 nm one.

Fractionation coefficients. Fractionation indices for 60 elements in a silicate NIST glass were first calculated by Fryer et al. in [12] relative to calcium as an internal standard (IS). The FIs were calculated as integrated signals for each element in the second half of continuous LS normalized to calcium divided by signals in the first half of LS normalized to calcium. Such FIs were measures of fractionation of each element in LS relative to the IS element. The value FI = 1 pointed to the absence of elemental fractionation under the experimental conditions. The FI values of elements in different matrices were distributed between three groups: for the majority of litophile elements forming sulfate, carbonate, phosphate, borate, and halide minerals, FI ~1; for many chalcophile elements forming the group of sulfide and telluride minerals, FI ~2 and higher; siderophile elements forming the major part of polymetallic ores were characterized by intermediate coefficients (Fig. 3).

FI were calculated later by other researchers, e.g., [28, 46, 48, 113, 114, 117, 129, 138, 139]. In [56], FI values determined in 130 fs LS at 785 nm were comparable with FI calculated by Fryer et al. [12] using a nanosecond 266 nm installation; however, for P, Cu, Zn, Ga, Ge, As, Se, Mo, Ag, Cd, In, Sn, Sb, W, Re, Au, Ti, Pb, and Bi with FI >1.5 at 266 nm ns LS [12], the FI values for NIR fs laser pulses were close to unity [56].

Significant elemental fractionation was found for Cu, Zn, Pb, P, Ga, Ge, Cd, Sb, Tl, and Bi: FI differed from 1 at 193 and 213 nm LS of silicate (NIST SRM 612), basalt (KL2-G), and carbonate (MACS-1) glasses [131]. A change in the diameter of laser spot from 20 to 110 μm led to a change in FI by 10–20%. A significant effect of the laser spot size on elemental fractionation was shown based on calculations of FI in brass and NIST samples [140].

In [129], FI values based on ^{42}Ca in UV fs LS–ICP–MS at the laser fluence ≤6 J/cm^2 in the average mass range (^{57}Fe ≤ m ≤ ^{111}Cd) strongly deviated from unity. The deviations of FI values were much smaller for fluences esceeded by far 6 J/cm^2. Chen et al. proposed a procedure for the correction of interelemental fractionation using the "internal standard normalized fractionation factor" for the calculation of analyte concentrations [114]. However, as follows from the work [141], FIs do not serve fundamental indicators of laser sampling, they strongly depend on the characteristics of laser irradiance and sample properties, and show only how masses of different elements are ablated during the formation of a crater in using specific characteristics.

In [71], FI values were determined for 11 NIST 610 isotopes in fs and ps LS–ICP–MS with different pulse frequencies. The largest deviation of FIs was observed at 10 and 5 Hz in fs and ps modes, respectively. An increase in frequency from 5 to 50 Hz reduced fractionation for all isotopes at both pulse durations. Machida et al observed changes in FIs with time for 34 elements [142]. Depending on the change in FIs, elements were divided into two groups. It was recommended to select an IS element from the group of elements to be determined. Luo et al. calculated FI values for 63 isotopes relative to calcium in 50-s intervals and showed that both types of elemental fractionation, from laser irradiance and in ICP, equally depended on the temperatures of element condensation [135].

Influence of laser operation parameters. In IR LS (1064 nm), in contrast to 266 nm LS, plasma screening of laser irradiance occurs and increases the risk of selective evaporation [43]. Substance fractionation,

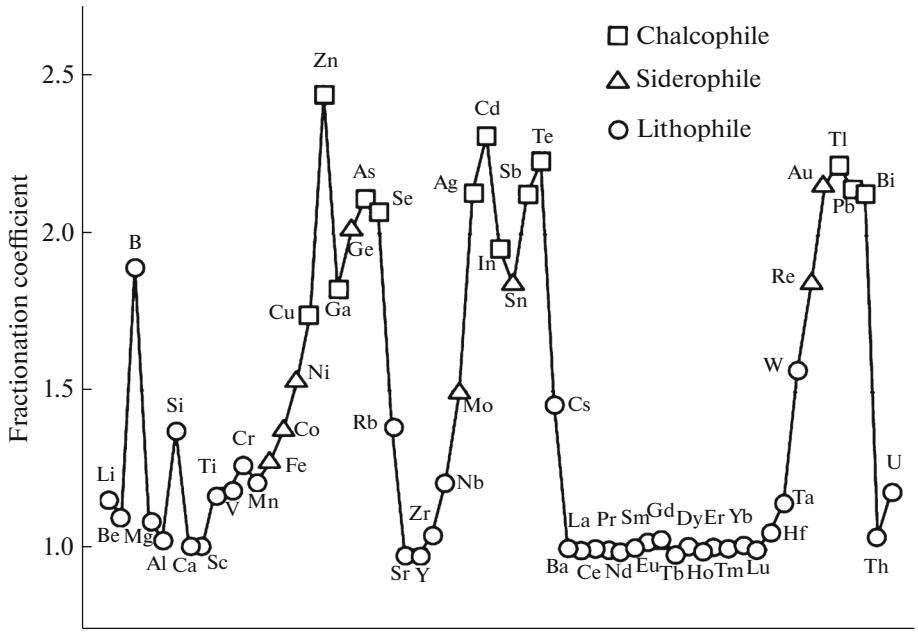

Fig. 3. Fractionation indices for 59 elements [1] (signs designate element assignment to the groups).

resulting in the poor representativity of the ablated sample [128], and a dependence of elemental fractionation on laser focusing (spot size), i.e., intensity of incident irradiance and melting points of element oxides [45], were observed. A significant increase in elemental fractionation for 14 elements with the reduction of the size of laser spot from 44 to 16 μm at a constant laser fluence was observed in natural silicates in contrast to NIST SRM 610-614, in which laser-induced elemental fractionation was quite insignificant [139]. The absence of elemental fractionation in LS at 266 nm and significant elemental fractionation in LS at 1064 and 532 nm, depending on laser focusing, allowed Figg et al. to conclude [45] that, in the last two cases, there was a local heating of the sample surface, which evaporated the most volatile elements and formed larger particles that did not decompose completely and were thermally extracted by more volatile elements in ICP. These and similar observations assume the use of UV irradiance with low pulse energies for gaining improved analytical results. The dependence of the selective evaporation of elements in LS on the frequency and power of laser pulses was shown in [124].

Jeffries et al. found a considerable reduction of fractionation with the improvement of analytical characteristics in UV ns LS at 266 nm in comparison with IR ns LS at 1064 nm [24]. On the contrary, Eggins et al. observed systematic elemental fractionation in LS at 193 nm and pulse duration of ~20 ns and drew a conclusion about the strong dependence of elemental fractionation on the energy and duration of laser pulses and about its probable independence of the wavelength of UV radiation [47]. For 6 ns LS with pulses at 266 and 213 nm, Liu et al. did not observe considerable distinctions in elemental fractionation [25]. In [49], elemental fractionation was observed for all three wavelengths of UV radiation, 157 nm (30 ns) and 213 and 266 nm (6 ns). The authors drew a conclusion that fractionation depends on the energy and number of laser pulses, i.e., for all wavelengths the researcher can select laser fluence at which fractionation is minimized or absolutely eliminated. However, a comparison of 193 and 266 nm nanosecond laser irradiance in [46, 48] has shown that elemental fractionation depends mainly on the wavelength of laser irradiance and is independent of the nature of the carrier gas (He or Ar). The elimination of elemental fractionation using 196 and 266 nm fs laser pulses was shown in [26, 65]. It was noted that element and isotope fractionation as the main restrictions of LS occur for nanosecond irradiance.

The study of elemental fractionation in fs LS–ICP–MS on binary metal and semiconductor samples and on multielement glasses in [143] was performed using successive single laser pulses. Fractionation was observed in the first laser pulses; it was quite significant at the laser fluence close to the LS threshold of samples. The ratio of elements in the ablated masses changed from one pulse to another to the achievement of a limiting fluence-independent value representing stoichiometric sampling. It was shown that limiting stoichiometric ratios could be attained with a smaller number of pulses if higher fluences were used. It was

also shown that elements with low first ionization potentials (**IP**s) are characterized by higher probabilities of LS, and in LS with almost equal IPs, fractionation was not observed or was very weak. A linear dependence of the depth of LS and crater diameter on the number of laser pulses in the fluence range 1.14–24.89 J/cm^2 was shown in [110].

As was shown in [23, 144], in the range of densities of incident radiation 0.6–2.0 GW/cm^2 in 5–6 ns LS, the fluctuation of element ratios of ablated mass was statistically insignificant.

Effect of crater geometry. The laser beam spatial energy profile is an important property determining the shape and morphology of LS craters. In a number of studies [e.g., 6, 42, 142, 143], it was noted that solid-state Nd:YAG lasers usually had Gaussian beam profiles, which could be easily focused on the target surface to a very small beam area, and the craters formed under these conditions were cone-shaped. However, the optical systems of the newest LS installations allowed the formation of beams with the top close to flat [42].

The number of laser pulses at their fixed positions on the sample also considerably affects the shape and depth of the forming craters, and consequently, the proceeding physical processes and elemental fractionation caused by these processes. A correlation between the geometry of LS pits and surface processes during LS (193 nm, 20 ns) was found in [47]. Fractionation was enhanced with the development of a crater [142] and became significant at actual radiation intensities below 0.2–0.3 GW/cm^2 [144]; however, the degree of fractionation was not directly related to the laser beam profile [6]. As was shown in [47, 144, 145], the degree of elemental fractionation became significant at the ratio of the width of an LS crater to its depth higher than six. An assumption was made in [25, 47] that the geometry of the crater affects elemental fractionation because of a contribution of plasma sampling and a decrease in irradiance efficiency during mass transfer. Russo et al. supposed that, at a proper choice of laser parameters and the ratio of crater sides, preferable evaporation and fractionation could be eliminated [146].

It was shown [147] that laser-induced elemental fractionation is a function of the number of laser pulses and is exponentially inversely proportional to the spot area. To minimize the fractionation of Pb/U, an increase in the LS spot size to ≥150 μm was used. The absence of fractionation effects was shown in the determination of trace elements in zeolites, basalt, and andesite, rare-earth elements in NIST SRM 612 glass by LS–ICP–MS (266 nm, 5 ns) at spot diameters of 200, 320, and 340 μm [148–150].

* * *

The LS–ICP–MS method provided analytical chemists with an efficient tool for elemental analysis and the determination of element and isotope ratios in different solid samples with limits of detection down to several ppm, high spatial resolution down to several μm, and without chemical sample preparation. The main contribution to the instability of the measurements is made by fractionation during the evaporation of chemical elements, associated with thermal processes in LS. The dependence of thermal processes on the wavelength, pulse duration, and power characteristics of laser irradiance, and also on the geometry of the crater and the ratio of its sides and the composition and properties of the sample was shown. The advantages of an UV laser over an IR one were revealed. They consist in the elimination of matrix effects, the reduction of spatial resolution up to 4 μm, higher sensitivity, and possibility of analyzing any solid sample. Shorter laser wavelengths ensure higher rates of ablation and lower degrees of elemental fractionation. At nanosecond pulses, thermal processes are prevailing mechanisms of matter ablation for particles of micron size, and, in fs LS, photomechanical mechanisms are prevailing, which lead to the matter ablation of particles with uniform and small particle size distribution, transferred by the gas stream without significant losses and completely ionized in ICP with the minimum total fractionation. Depending on the characteristics of laser irradiance and sample properties, fs LS–ICP–MS exceeds the ns version in sensitivity by approximately one order of magnitude. The UV fs LS–ICP–MS method is substantially independent of matrix effects, which favors use in the analysis of standard samples without matrix matching. A measure of elemental fractionation in laser sampling relatively to an internal standard element is provided by fractionation indices.

ACKNOWLEDGMENTS

This work was partially supported by the Ministry of Education and Science of the Russian Federation within the Program of Increasing the Competitiveness of NUST MISiS among the Leading World Scientific and Educational Centers for 2013–2020, project no. K1-2014-026 and Russian Science Foundation, project no. 14-13-00897.

We are profoundly grateful to V.K. Karandashev for valuable remarks and fruitful discussion of the work in manuscript preparation.

REFERENCES

1. Günther, D., Jackson, S.E., and Longerich, H.P., *Spectrochim. Acta, Part B*, 1999, vol. 54, no. 3, p. 381.
2. Durrant, S., *J. Anal. At. Spectrom.*, 1999, vol. 14, no. 9, p. 1385.
3. Winefordner, J.D., Gornushkin, I.B., Pappas, D., Matveev, O.I., and Smith, B.W., *J. Anal. At. Spectrom.*, 2000, vol. 15, no. 9, p. 1161.

4. Günther, D., Horn, I., and Hattendorf, B., *Fresenius' J. Anal. Chem*., 2000, vol. 368, no. 1, p. 4.
5. Russo, R.E., Mao, X., and Borisov, O.V., *TrAC, Trends Anal. Chem*., 1998, vol. 17, no. 8, p. 461.
6. Russo, R.E., Mao, X., Liu, H., Gonzalez, J., and Mao, S.S., *Talanta*, 2002, vol. 57, no. 3, p. 425.
7. Rodriguez, H.B., Lozano, D.O., Martínez, Y.A.R., Alcázar, G.A.P., Flege, S., Balogh, A.G., Cabri, L.J., and Tubrett, M., *Hyperfine Interact.*, 2007, vol. 175, nos. 1–3, p. 195.
8. Gray, A.L., *Analyst*, 1985, vol. 110, no. 5, p. 551.
9. Arrowsmith, P., *Anal. Chem.*, 1987, vol. 59, no. 10, p. 1437.
10. Jackson, S.E., Longerich, H.P., Dunning, G.R., and Fryer, B.J., *Can. Mineral.*, 1992, vol. 30, p. 1049.
11. Chenery, S. and Cook, J.M., *J. Anal. At. Spectrom.*, 1993, vol. 8, no. 2, p. 299.
12. Fryer, B.J., Jackson, S.E., and Longerich, H.P., *Can. Mineral.*, 1995, vol. 33, p. 303.
13. Günther, D., Frischknecht, R., Heinrich, C.A., and Kahlert, H.J., *J. Anal. At. Spectrom.*, 1997, vol. 12, no. 9, p. 939.
14. Eggins, S.M., Rudnick, R.L., and McDonough, W.F., *Earth. Planet. Sci. Lett.*, 1998, vol. 154, no. 1, p. 53.
15. Pearce, N.J., Perkins, W.T., Abell, I., Duller, G.A., and Fuge, R., *J. Anal. At. Spectrom.*, 1992, vol. 7, no. 1, p. 53.
16. Longerich, H.P., Jackson, S.E., Fryer, B.J., and Strong, D.F., *Geosci. Can.*, 1993, vol. 20, no. 1, p. 21.
17. Cromwell, E.F. and Arrowsmith, P., *Anal. Chem.*, 1995, vol. 67, no. 1, p. 131.
18. Günther, D., Longerich, H.P., Forsythe, L., and Jackson, S.E., *Am. Lab.*, 1995, vol. 27, p. 24.
19. Fuge, R., Palmer, T.J., Pearce, N.J., and Perkins, W.T., *Appl. Geochem.*, 1993, vol. 8, p. 111.
20. Denoyer, E.R., Fredeen, K.J., and Hager, J.W., *Anal. Chem.*, 1991, vol. 63, no. 8, p. 445.
21. Jeffries, T.E., Perkins, W.T., and Pearce, N.J.G., *Analyst*, 1995, vol. 120, no. 5, p. 1365.
22. Mochizuki, T., Sakashita, A., Iwata, H., Kagaya, T., Shimamura, T., and Blair, P., *Anal. Sci.*, 1988, vol. 4, no. 4, p. 403.
23. Radziemski, L.J., *Microchem. J.*, 1994, vol. 50, no. 3, p. 218.
24. Jeffries, T.E., Pearce, N.J.G., Perkins, W.T., and Raith, A., *Anal. Commun.*, 1996, vol. 33, no. 1, p. 35.
25. Liu, H., Borisov, O.V., Mao, X., Shuttleworth, S., and Russo, R.E., *Appl. Spectrosc.*, 2000, vol. 54, no. 10, p. 1435.
26. Horn, I., von Blanckenburg, F., Schoenberg, R., Steinhoefel, G., and Markl, G., *Geochim. Cosmochim. Acta*, 2006, vol. 70, no. 14, p. 3677.
27. Stafe, M., Marcu, A., and Puscas, N.N., *Pulsed Laser Ablation of Solids*, Heidelberg: Springer, 2014.
28. Russo, R.E., Mao, X., Gonzalez, J.J., and Mao, S.S., *J. Anal. At. Spectrom.*, 2002, vol. 17, no. 9, p. 1072.
29. Russo, R.E., Mao, X., and Mao, S.S., *Anal. Chem.*, 2002, vol. 74, no. 3, p. 70.
30. *Ion, J., Laser Processing of Engineering Materials: Principles, Procedure and Industrial Application*, Butterworth-Heinemann, 2005.
31. Fernández, B., Claverie, F., Pécheyran, C., and Donard, O.F., *TrAC, Trends Anal. Chem.*, 2007, vol. 26, no. 10, p. 951.
32. Koch, J. and Günther, D., *Appl. Spectrosc.*, 2011, vol. 65, no. 5, p. 155.
33. *Inductively Coupled Plasma Spectrometry and Its Applications*, Hill, S.J., Ed., Oxford: Blackwell, 2007, 2nd ed.
34. Jarvis, K.E., Gray, A.L., and Houk, R.S., *Handbook of ICP–MS*, Glasgow: Blackie and Son, 1992.
35. *ICP Mass Spectrometry Handbook*, Nelms, S.M., Ed., Oxford: Blackwell, 2005.
36. Becker, S., *Inorganic Mass Spectrometry: Principles and Applications*, Chichester: Wiley, 2007.
37. Gackle, M. and Merten, D., *Spectrochim. Acta, Part B*, 2010, vol. 65, no. 12, p. 991.
38. Gray, A.L. and Date, A.R., *Analyst*, 1983, vol. 108, no. 1290, p. 1033.
39. Houk, R.S., Fassel, V.A., Flesch, G.D., Svec, H.J., Gray, A.L., and Taylor, C.E., *Anal. Chem.*, 1980, vol. 52, no. 14, p. 2283.
40. Date, A.R. and Gray, A.L., *Analyst*, 1981, vol. 106, no. 1269, p. 1255.
41. Henry, R. and Cassel, T., in *The Handbook of Metabolomics: Methods in Pharmacology and Toxicology*, Fan, T.W.M., Lane, A.N., and Higashi, R.M, Eds., New York: Springer, 2012, vol. 17, p. 99.
42. Shaheen, M.E., Gagnon, J.E., and Fryer, B.J., *Chem. Geol.*, 2012, vol. 330, p. 260.
43. Geertsen, C., Briand, A., Chartier, F., Lacour, J.L., Mauchien, P., Sjöström, S., and Mermet, J.M., *J. Anal. At. Spectrom.*, 1994, vol. 9, no. 1, p. 17.
44. Cahoon, E.M. and Almirall, J.R., *Appl. Opt.*, 2010, vol. 49, no. 13, p. 49.
45. Figg, D. and Kahr, M.S., *Appl. Spectrosc.*, 1997, vol. 51, no. 8, p. 1185.
46. Jeffries, T., Jackson, S., and Longerich, H., *J. Anal. At. Spectrom.*, 1998, vol. 13, no. 9, p. 935.
47. Eggins, S.M., Kinsley, L.P.J., and Shelley, J.M.G., *Appl. Surf. Sci.*, 1998, vol. 127, p. 278.
48. Günther, D. and Heinrich, C.A., *J. Anal. At. Spectrom.*, 1999, vol. 14, no. 9, p. 1369.
49. Russo, R.E., Mao, X.L., Borisov, O.V., and Liu, H., *J. Anal. At. Spectrom.*, 2000, vol. 15, no. 9, p. 1115.
50. Telouk, P., Rose-Koga, E.F., and Albarede, F., *Geostand. Newsl.*, 2003, vol. 27, no. 1, p. 5.
51. Guillong, M., Horn, I., and Günther, D., *J. Anal. At. Spectrom.*, 2003, vol. 18, no. 10, p. 1224.
52. Shannon, M.A., Mao, X.L., Fernandez, A., Chan, W.T., and Russo, R.E., *Anal. Chem.*, 1995, vol. 67, no. 24, p. 4522.
53. Mao, X.L., Ciocan, A.C., and Russo, R.E., *Appl. Spectrosc.*, 1998, vol. 52, no. 7, p. 913.
54. Le Harzic, R., Breitling, D., Weikert, M., Sommer, S., Föhl, C., Valette, S., Donnet, C., Audouard, E., and Dausinger, F., *Appl. Surf. Sci.*, 2005, vol. 249, no. 1, p. 322.

55. Perdian, D.C., Bajic, S.J., Baldwin, D.P., and Houk, R.S., *J. Anal. At. Spectrom.*, 2008, vol. 23, p. 325.
56. Shaheen, M., Gagnon, J.E., Yang, Z., and Fryer, B.J., *J. Anal. At. Spectrom.*, 2008, vol. 23, no. 12, p. 1610.
57. Freydier, R., Candaudap, F., Poitrasson, F., Arbouet, A., Chatel, B., and Dupré, B., *J. Anal. At. Spectrom.*, 2008, vol. 23, no. 5, p. 702.
58. Wohlgemuth-Ueberwasser, C.C. and Jochum, K.P., *J. Anal. At. Spectrom.*, 2015, vol. 30, no. 12, p. 2469.
59. Poitrasson, F., Mao, X., Mao, S.S., Freydier, R., and Russo, R.E., *Anal. Chem.*, 2003, vol. 75, no. 22, p. 6184.
60. d'Abzac, F.X., Poitrasson, F., Freydier, R., and Seydoux-Guillaume, A.M., *J. Anal. At. Spectrom.*, 2010, vol. 25, no. 5, p. 681.
61. Ohata, M., Tabersky, D., Glaus, R., Koch, J., Hattendorf, B., and Günther, D., *J. Anal. At. Spectrom.*, 2014, vol. 29, no. 8, p. 1345.
62. Steinhoefel, G., Horn, I., and von Blanckenburg, F., *Chem. Geol.*, 2009, vol. 268, no. 1, p. 67.
63. Steinhoefel, G., Horn, I., and von Blanckenburg, F., *Geochim. Cosmochim. Acta*, 2009, vol. 73, no. 18, p. 5343.
64. Steinhoefel, G., von Blanckenburg, F., Horn, I., Konhauser, K.O., Beukes, N.J., and Gutzmer, J., *Geochim. Cosmochim. Acta*, 2010, vol. 74, no. 9, p. 2677.
65. Horn, I. and von Blanckenburg, F., *Spectrochim. Acta, Part B*, 2007, vol. 62, no. 4, p. 410.
66. Košler, J., Pedersen, R.B., Kruber, C., and Sylvester, P.J., *J. Anal. At. Spectrom.*, 2005, vol. 20, no. 3, p. 192.
67. Jackson, S.E. and Günther, D., *J. Anal. At. Spectrom.*, 2003, vol. 18, no. 3, p. 205.
68. Horn, I., Schoenberg, R., and von Blanckenburg, F., *J. Anal. At. Spectrom.*, 2006, vol. 21, no. 2, p. 211.
69. Steinhoefel, G., Breuer, J., von Blanckenburg, F., Horn, I., Kaczorek, D., and Sommer, M., *Chem. Geol.*, 2011, vol. 286, no. 3, p. 280.
70. Shaheen, M.E., Gagnon, J.E., and Fryer, B.J., *J. Appl. Phys.*, 2013, vol. 114, no. 8, 083110. doi doi 10.1063/1.4808455
71. Shaheen, M.E., Gagnon, J.E., and Fryer, B.J., *Spectrochim. Acta, Part B*, 2015, vol. 107, p. 97. doi doi 10.1016/j.sab.2015.02.010
72. Mao, S.S., Mao, X., Greif, R., and Russo, R.E., *Appl. Phys. Lett.*, 2000, vol. 76, no. 23, p. 3370.
73. Mao, S.S., Mao, X., Greif, R., and Russo, R.E., *Appl. Phys. Lett.*, 2000, vol. 77, no. 16, p. 2464.
74. Chichkov, B.N., Momma, C., Nolte, S., Von Alvensleben, F., and Tünnermann, A., *Appl. Phys. A*, 1996, vol. 63, no. 2, p. 109.
75. Wang, X.Y., Riffe, D.M., Lee, Y.S., and Downer, M.C., *Phys. Rev. B: Condens. Matter Mater. Phys.*, 1994, vol. 50, no. 11, p. 8016.
76. Schoenlein, R.W., Lin, W.Z., Fujimoto, J.G., and Eesley, G.L., *Phys. Rev. Lett.*, 1987, vol. 58, no. 16, p. 1680.
77. Fann, W.S., Storz, R., Tom, H.W.K., and Bokor, J., *Phys. Rev. B: Condens. Matter Mater. Phys.*, 1992, vol. 46, no. 20, p. 13592.
78. Stuart, B.C., Feit, M.D., Rubenchik, A.M., Shore, B.W., and Perry, M.D., *Phys. Rev. Lett.*, 1995, vol. 74, no. 12, p. 2248.
79. Ihlemann, J., Scholl, A., Schmidt, H., and Wolff-Rottke, B., *Appl. Phys. A*, 1995, vol. 60, no. 4, p. 411.
80. Mao, S.S., Mao, X.L., Greif, R., and Russo, R.E., *Appl. Surf. Sci.*, 1998, vol. 127, p. 206.
81. La Haye, N.L., Harilal, S.S., Diwakar, P.K., and Hassanein, A., *J. Anal. At. Spectrom.*, 2013, vol. 28, no. 11, p. 1781.
82. Kelly, R. and Miotello, A., *Appl. Surf. Sci.*, 1996, vol. 96, p. 205.
83. Kelly, R. and Miotello, A., *Nucl. Instrum. Methods Phys. Res., Sect. B*, 1997, vol. 122, no. 3, p. 374.
84. Miotello, A. and Kelly, R., *Appl. Phys. Lett.*, 1995, vol. 67, no. 24, p. 3535.
85. Miotello, A. and Kelly, R., *Appl. Phys. A*, 1999, vol. 69, no. 1, p. 67.
86. Lu, Q., Mao, S.S., Mao, X., and Russo, R.E., *Appl. Phys. Lett.*, 2002, vol. 80, no. 17, p. 3072.
87. Yoo, J.H., Borisov, O.V., Mao, X., and Russo, R.E., *Anal. Chem.*, 2001, vol. 73, no. 10, p. 2288.
88. Yoo, J.H., Jeong, S.H., Greif, R., and Russo, R.E., *J. Appl. Phys.*, 2000, vol. 88, no. 3, p. 1638.
89. Yoo, J.H., Jeong, S.H., Mao, X.L., Greif, R., and Russo, R.E., *Appl. Phys. Lett.*, 2000, vol. 76, no. 6, p. 783.
90. Mao, X. and Russo, R.E., *Appl. Phys. A*, 1997, vol. 64, no. 1, p. 1.
91. Liu, H.C., Mao, X.L., Yoo, J.H., and Russo, R.E., *Spectrochim. Acta, Part B*, 1999, vol. 54, no. 11, p. 1607.
92. Phipps, C.R. and Dreyfus, R.W., in Laser Ionization Mass Analysis, Vertes, A., Gijbels, R., and Adams, F., Eds., New York: Wiley, 1993, p. 369.
93. Singh, R.K. and Viatella, J., *J. Appl. Phys.*, 1994, vol. 75, no. 2, p. 1204.
94. Amoruso, S., Bruzzese, R., Spinelli, N., and Velotta, R., *J. Phys. B*, 1999, vol. 32, no. 14, p. R131.
95. Schäfer, C., Urbassek, H.M., and Zhigilei, L.V., *Phys. Rev. B: Condens. Matter Mater. Phys.*, 2002, vol. 66, no. 11, p. 115404.
96. Zhigilei, L.V., *Appl. Phys. A*, 2003, vol. 76, no. 3, p. 339.
97. Marla, D., Bhandarkar, U.V., and Joshi, S.S., *J. Appl. Phys.*, 2011, vol. 109, no. 2, 021101. doi doi 10.1063/1.3537838
98. Mao, X.L., Chan, W.T., Shannon, M.A., and Russo, R.E., *J. Appl. Phys.*, 1993, vol. 74, no. 8, p. 4915.
99. Kuhn, H.R. and Günther, D., *J. Anal. At. Spectrom.*, 2004, vol. 19, no. 9, p. 1158.
100. Koch, J., Lindner, H., Von Bohlen, A., Hergenroder, R., and Niemax, K., *J. Anal. At. Spectrom.*, 2005, vol. 20, no. 9, p. 901.
101. Zhigilei, L.V., Lin, Z., and Ivanov, D.S., J. Phys. Chem. C, 2009, vol. 113, no. 27, p. 11892.
102. Le Harzic, R., Stracke, F., and Zimmermann, H., *J. Appl. Phys.*, 2013, vol. 113, no. 18, 183503. doi doi 10.1063/1.4803895
103. Bian, Q., Garcia, C.C., Koch, J., and Niemax, K., *J. Anal. At. Spectrom.*, 2006, vol. 21, no. 2, p. 187.

104. Pisonero, J., Fernandez, B., and Günther, D., *J. Anal. At. Spectrom.*, 2009, vol. 24, no. 9, p. 1145.
105. Garcia, C.C., Lindner, H., and Niemax, K., *J. Anal. At. Spectrom.*, 2009, vol. 24, no. 1, p. 14.
106. Song, K.H. and Xu, X., *Appl. Phys. A*, 1997, vol. 65, no. 4, p. 477.
107. Song, K.H. and Xu, X., *Appl. Surf. Sci.*, 1998, vol. 127, p. 111.
108. Xu, X., Chen, G., and Song, K.H., *Int. J. Heat Mass Transfer*, 1999, vol. 42, no. 8, p. 1371.
109. Xu, X. and Song, K.H., *Mater. Sci. Eng., A*, 2000, vol. 292, no. 2, p. 162.
110. Shaheen, M.E. and Fryer, B.J., *Laser Part. Beams*, 2012, vol. 30, p. 473.
111. Jeong, S.H., Borisov, O.V., Yoo, J.H., Mao, X.L., and Russo, R.E., *Anal. Chem.*, 1999, vol. 71, no. 22, p. 5123.
112. Hirata, T. and Nesbitt, R.W., *Geochim. Cosmochim. Acta*, 1995, vol. 59, no. 12, p. 2491.
113. Borisova, A.Y., Freydier, R., Polve, M., Salvi, S., Candaudap, F., and Aigouy, T., *Geostand. Geoanal. Res.*, 2008, vol. 32, no. 2, p. 209.
114. Chen, Z., *J. Anal. At. Spectrom.*, 1999, vol. 14, no. 12, p. 1823.
115. Motelica-Heino, M. and Donard, O.F., *Geostand. Newsl.*, 2001, vol. 25, nos. 2–3, p. 345.
116. Motelica-Heino, M., Le Coustumer, P., and Donard, O.F.X., *J. Anal. At. Spectrom.*, 2001, vol. 16, no. 6, p. 542.
117. Kroslakova, I. and Günther, D., *J. Anal. At. Spectrom.*, 2007, vol. 22, no. 1, p. 51.
118. Votyakov, S.L. and Adamovich, N.N., *Litosfera*, 2011, no. 4, p. 56.
119. Russo, R.E., *Appl. Spectrosc.*, 1995, vol. 49, no. 9, p. 14.
120. Chan, W.T., Mao, X.L., and Russo, R.E., *Appl. Spectrosc.*, 1992, vol. 46, no. 6, p. 1025.
121. Leloup, C., Marty, P., Dall'ava, D., and Perdereau, M., *J. Anal. At. Spectrom.*, 1997, vol. 12, no. 9, p. 945.
122. Mao, X., Chan, W.T., Caetano, M., Shannon, M.A., and Russo, R.E., *Appl. Surf. Sci.*, 1996, vol. 96, p. 126.
123. Cromwell, E.F. and Arrowsmith, P., *Appl. Spectrosc.*, 1995, vol. 49, no. 11, p. 1652.
124. Mochizuki, T., Sakashita, A., Tsuji, T., Iwata, H., Ishibashi, Y., and Gunji, N., *Anal. Sci.*, 1991, vol. 7, p. 479.
125. Longerich, H.P., Günther, D., and Jackson, S.E., *Fresenius' J. Anal. Chem.*, 1996, vol. 355, nos. 5–6, p. 538.
126. Outridge, P.M., Doherty, W., and Gregoire, D.C., *Spectrochim. Acta, Part B*, 1997, vol. 52, no. 14, p. 2093.
127. Russo, R.E., Mao, X.L., Chan, W.T., Bryant, M.F., and Kinard, W.F., *J. Anal. At. Spectrom.*, 1995, vol. 10, no. 4, p. 295.
128. Shuttleworth, S., *Appl. Surf. Sci.*, 1996, vol. 96, p. 513.
129. Koch, J., Walle, M., Pisonero, J., and Günther, D., *J. Anal. At. Spectrom.*, 2006, vol. 21, no. 9, p. 932.
130. Loewen, M.W. and Kent, A.J., *J. Anal. At. Spectrom.*, 2012, vol. 27, no. 9, p. 1502.
131. Jochum, K.P., Scholz, D., Stoll, B., Weis, U., Wilson, S.A., Yang, Q., Schwalb, A., Borner, N., Jacob, D.E., and Andreae, M.O., *Chem. Geol.*, 2012, vol. 318, p. 31.
132. Liu, C., Mao, X.L., Mao, S.S., Zeng, X., Greif, R., and Russo, R.E., *Anal. Chem.*, 2004, vol. 76, no. 2, p. 379.
133. Guillong, M. and Günther, D., *J. Anal. At. Spectrom.*, 2002, vol. 17, no. 8, p. 831.
134. Jorgensen, D.J., Titus, M.S., and Pollock, T.M., *Appl. Surf. Sci.*, 2015, vol. 353, p. 700.
135. Luo, T., Wang, Y., Hu, Z., Günther, D., Liu, Y., Gao, S., Li, M., and Hu, S., *J. Anal. At. Spectrom.*, 2015, vol. 30, no. 4, p. 941.
136. Guillong, M., Kuhn, H.R., and Günther, D., *Spectrochim. Acta, Part B*, 2003, vol. 58, no. 2, p. 211.
137. Hathorne, E.C., James, R.H., Savage, P., and Alard, O., *J. Anal. At. Spectrom.*, 2008, vol. 23, no. 2, p. 240.
138. Diwakar, P.K., Gonzalez, J.J., Harilal, S.S., Russo, R.E., and Hassanein, A., *J. Anal. At. Spectrom.*, 2014, vol. 29, no. 2, p. 339.
139. Hu, Z., Liu, Y., Chen, L., Zhou, L., Li, M., Zong, K., Zhu, L., and Gao, S., *J. Anal. At. Spectrom.*, 2011, vol. 26, no. 2, p. 425.
140. Diwakar, P.K., Harilal, S.S., Hassanein, A., and Phillips, M.C., *J. Appl. Phys.*, 2014, vol. 116, no. 13, 133301. doi 10.1063/1.4896169
141. Gonzalez, J., Mao, X.L., Roy, J., Mao, S.S., and Russo, R.E., *J. Anal. At. Spectrom.*, 2002, vol. 17, no. 9, p. 1108.
142. Machida, R., Nakazawa, T., and Furuta, N., *Anal. Sci.*, 2015, vol. 31, no. 5, p. 345.
143. Garcia, C.C., Lindner, H., von Bohlen, A., Vadla, C., and Niemax, K., *J. Anal. At. Spectrom*, 2008, vol. 23, no. 4, p. 470.
144. Borisov, O.V., Mao, X., and Russo, R.E., *Spectrochim. Acta, Part B*, 2000, vol. 55, no. 11, p. 1693.
145. Mank, A.J. and Mason, P.R., *J. Anal. At. Spectrom.*, 1999, vol. 14, no. 8, p. 1143.
146. Russo, R.E., Mao, X., Gonzalez, J.J., and Yoo, J., *Spectroscopy*, 2013, vol. 28, no. 1, p. 24.
147. Horn, I., Rudnick, R.L., and McDonough, W.F., *Chem. Geol.*, 2000, vol. 164, no. 3, p. 281.
148. Becker, J.S., Pickhardt, C., and Dietze, H.J., *Microchim. Acta*, 2000, vol. 135, nos. 1–2, p. 71.
149. Pickhardt, C., Brenner, I.B., Becker, J.S., and Dietze, H.J., *Fresenius' J. Anal. Chem.*, vol. 368, no. 1, p. 79.
150. Pickhardt, C., Becker, J.S., and Dietze, H.J., *Fresenius' J. Anal. Chem.*, 2000, vol. 368, nos. 2–3, p. 173.

Translated by E. Rykova